Robust Formation Control Of Wheeled Non-Holonomic Robots Via Predictive Sliding Mode Control

Damani Allaeddine Yahia[1], Bachir Nail[2]

[1]*Laboratory of signal and image processing, Saad Dahlab University Blida 1, Blida, Algeria*

[2]*Renewable Energy Systems Applications Laboratory (LASER), Faculty of Sciences and Technology, Ziane Achour University, Djelfa, Algeria.*

Abstract

This paper presents the design of a kinematic controller for coordinating a team of mobile robots into specified formation configurations using the leader-follower framework. First, the leader-follower strategy is reformulated as a trajectory tracking problem. Then, a discrete model predictive control (DMPC) is integrated with a discrete sliding mode (DSM) control to guide the follower robots in tracking the leader's trajectory while preserving the required formation geometric configuration. The suggested control scheme ensures precise trajectory tracking and a robust formation maintenance with a constrained and chattering free control inputs. Simulation results demonstrate the effectiveness, efficiency, and practicality of the proposed control strategy for real-world scenarios.

Keywords

Mobile Robots, Predictive Control, Formation Control, Sliding Mode, Leader Follower Approach

1. Introduction

Formation control is a fundamental aspect of multi-robot systems, it allows for the robots to operate cohesively by regulating states like position and orientation to achieve specific geometric configurations. Its broad applicability spans various domains such as exploration, rescue missions, surveillance, and transportation, which make it a critical focus in robotics research. Recent developments in the field have led to the exploration of various control methodologies, including behavior-based [1, 2], leader-follower[3, 4] and virtual structure [5, 6, 7] approaches. In the existing literature, researchers have applied a range of control techniques to implement formation control in wheeled nonholonomic mobile robots, leveraging the leader-follower framework. These techniques include graph theory approaches [8, 9, 10], consensus algorithms [11, 12, 13], SMC sliding mode control [14, 15], MPC model predictive control [16, 17, 18, 19], PID control [20, 21] and reinforcement learning [22, 23, 24, 25].

Among this control schemes, sliding mode control (SMC) approaches have been widely adopted in formation control of mobile robots. primarily due to its appealing attributes, such as finite-time convergence and resilience against perturbations and uncertainties. However, the chattering phenomenon resulting from the reaching law, and its corresponding high control effort, stands as its primary limitation, which have inspired substantial

research to address these issue. For example, authors in [26] addressed the formation control of nonholonomic mobile robots. a globally finite-time stable sliding mode controller has been designed. Then, a continuous reaching law has been derived to mitigate the chattering caused by control limitations and computation time delays. In [27] a second order sliding mode controller has been developed , based on the relative motion states and without the leader velocity measurement, to stabilize the robots towards the required time-varying formation and to avoid the the chattering phenomena. The authors in [28] design a sliding mode formation controller for differential drive robots. They used a novel approach inspired by immune regulation mechanisms, coupled with fuzzy boundary layer method. To reduce the chattering and to compensate uncertainty without requiring prior knowledge of its boundaries. In [29] a tracking control method for multiple robots has been presented. A sliding mode controller has been introduced to asymptotically stabilize the robots into the required formation. To address the velocity jump issue, authors incorporates a novel sliding mode approach based on the neural dynamic model[30, 31, 32].

On the other hand, employing model predictive control MPC for the formation control of nonholonomic mobile robots can effectively account for physical limits of the robots, making it capable for yielding an optimal formation tracking and maintenance. The authors in [33] used a virtual robot as a leader, then an MPC method is applied to the followers to accomplish the leader-follower formation objective based on two models. Novel terminal state regions and controllers are developed to assure the stability of the controller.

In [34] a multi-robot systems was controlled using a cooperative CCEA coevolutionary algorithm based MPC approach. To predict the future states, they utilized the past state values of the robots, rather than their current values. And the asymptotic stability has been guaranteed, by tuning the sampling period and choosing suitable constraints of the states and inputs[35, 36, 37]. The authors in [38] suggested an MPC controller for a leader follower formation based on the separation-bearing-orientation scheme. the particle swarm algorithm is employed for solving the optimization problem, where the global solution is considered as the control input.

The key contribution of this paper lies in the development of a controller that combines discrete model predictive control MPC and discrete sliding mode control to achieve a robust and accurate formation control of nonholonomic wheeled mobile robots. The integration of MPC allows for optimal formation producing and tracking with constrained states and inputs, while the sliding mode control ensures robustness against kinematic perturbations subjected to the robots model in practice. By leveraging the strengths of both control techniques, the proposed method aims to improve the overall formation control performances. To evaluate the effectiveness of suggested control method, simulation examples are conducted. Where a comparison is made between the performance of the proposed method and conventional discrete sliding mode control technique. The results clearly demonstrate the superior performance of the proposed method.

2. Problem Formulation

2.1. Nonholonomic mobile robot kinematic model

Consider the differential-drive wheeled mobile robot shown in Figure 1. Let $q = [x\ y\ \theta]^T$ be the robot center of mass posture, where (x, y) denotes the position of the robot in the global Cartesian frame (OXY) and θ is the orientation angle.

This robot satisfy the following pure rolling and non-slipping nonholonomic constraints given by:

$$\dot{y}\cos\theta - \dot{x}\sin\theta = 0 \tag{1}$$

By using the nonholonomic constraints in (1), the kinematic model of the robot can be described as follow:

$$\dot{q} = \begin{bmatrix} \cos\theta & 0 \\ \sin\theta & 0 \\ 0 & 1 \end{bmatrix} \begin{bmatrix} \nu \\ \omega \end{bmatrix} = J(q)u \tag{2}$$
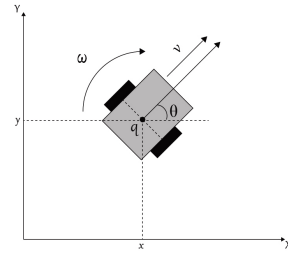

Figure 1: Differential-drive wheeled mobile robot.

Where ω is the robot angular velocity and ν is the robot linear velocity.

In practice, the robot model is subjected to kinematic uncertainty and input disturbances. Hence, a more realistic model of the robot can be expressed as follow [39]:

$$\dot{q} = J(q)(u + \Delta) \tag{3}$$

Where $\Delta = [\delta_\nu\ \delta_\omega]^T$ denotes the unknown input disturbances, and its assumed to be upper bounded by [39]:

$$|\Delta| \leq \gamma$$

where γ is a positive constant.

2.2. Leader follower formation model

Figure 2 show the basic architecture of the leader-follower formation approach. Where the posture of the leader robot R_l is $q_l = [x_l\ y_l\ \theta_l]^T$ and the posture of the follower robot R_f is given by $q_f = [x_f\ y_f\ \theta_f]^T$ and the desired posture for the follower robot is given by $q_d = [x_d\ y_d\ \theta_d]^T$.

The leader-follower approach can be seen as a trajectory tracking problem where the follower robot must track the trajectories generated by the leader robot in-order to preserve the required separation distance L_d and heading angle Φ_d, and to form the predefined formation shape. Hence the desired posture q_d can be given as [40]:

$$q_d = \begin{bmatrix} x_d \\ y_d \\ \theta_d \end{bmatrix} = \begin{bmatrix} x_l + L_d\cos(\Phi_d + \theta_l) \\ y_l + L_d\sin(\Phi_d + \theta_l) \\ \text{atan2}(\dot{y}_d, \dot{x}_d + \kappa\pi) \end{bmatrix} \tag{4}$$

Where $k = 0, 1$ is the driving direction (0 for the forward motion and 1 for reverse) and $atan2$ is the four-quadrant inverse tangent function. To accomplish the
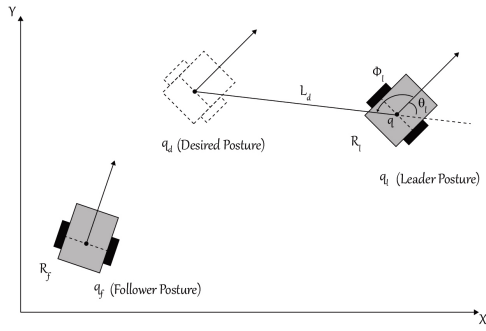
Figure 2: Leader-Follower Formation Structure.

formation objective, the follower robot need to follow the reference trajectory consist of the set of the desired postures q_d, which implies that the following must satisfy:

$$\lim_{t \to \infty} (q_d - q_f) = 0 \qquad (5)$$

2.3. Leader follower formation error dynamics

Since the leader-follower formation is converted to a trajectory tracking problem, the tracking error model of the formation can be written as:

$$e = \begin{bmatrix} x_e \\ y_e \\ \theta_e \end{bmatrix} = \begin{bmatrix} \cos\theta & \sin\theta & 0 \\ -\sin\theta & \cos\theta & 0 \\ 0 & 0 & 1 \end{bmatrix} \begin{bmatrix} x_d - x_f \\ y_d - y_f \\ \theta_d - \theta_f \end{bmatrix} \qquad (6)$$

The tracking error dynamics of the formation can be obtained by taking the time derivative of (6) and by using equations (3) and (1) as follow [41]:

$$\dot{e} = \begin{bmatrix} \cos\theta_f & 0 \\ \sin\theta_f & 0 \\ 0 & 1 \end{bmatrix} \begin{bmatrix} v_d \\ \omega_d \end{bmatrix} + \begin{bmatrix} -1 & y_e \\ 0 & -x_e \\ 0 & -1 \end{bmatrix} \begin{bmatrix} u + \Delta \end{bmatrix} (7)$$

Where v_d and ω_d are the linear and angular feedforward control input defined as:

$$\begin{cases} v_d = \pm\sqrt{\dot{x}_d^2 + \dot{y}_d^2} \\ \omega_d = \frac{\dot{x}_d\ddot{y}_d - \dot{y}_d\ddot{x}_d}{\dot{x}_d^2 + \dot{y}_d^2} \end{cases} \qquad (8)$$

Where $(+)$ for the forward motion and $(-)$ for backward motion . By neglecting the input disturbance $\Delta = \begin{bmatrix} \delta_{\nu_f} & \delta_{\omega_f} \end{bmatrix}^T$, then defining the control input vector of the follower robot u as the sum of the feedforward and feedback control action:

$$u = u_d + u_c \qquad (9)$$

Where $u_d = \begin{bmatrix} v_d \cos\theta_e & \omega_d \end{bmatrix}^T$ is the feedforward control vector and $u_c = \begin{bmatrix} u_{c1} & u_{c2} \end{bmatrix}^T$ is the feedback vector input.

Assuming $\Delta = 0$ and substituting (9) into equation (7), gives the following tracking error dynamics :

$$\begin{aligned} \dot{x}_e &= \omega_d y_e - u_{c1} + u_{c2} y_e \\ \dot{y}_e &= v_d \sin\theta_e - \omega_d x_e - u_{c2} x_e \\ \dot{\theta}_e &= -u_{c2} \end{aligned} \qquad (10)$$

Using (9) and linearizing (10) around ($x_e = y_e = \theta_e = 0$ and $u_{c1} = u_{c2} = 0$) results the following linear model [42] :

$$\dot{e} = \begin{bmatrix} 0 & \omega_d & 0 \\ -\omega_d & 0 & v_d \\ 0 & 0 & 0 \end{bmatrix} e + \begin{bmatrix} -1 & 0 \\ 0 & 0 \\ 0 & -1 \end{bmatrix} u_c \quad (11)$$

Which can be written in a state-space form as:

$$\dot{e}(t) = A_c(t)e(t) + B_c u_c(t) \qquad (12)$$

3. Discrete predictive sliding mode control

3.1. Discrete sliding mode control design

The linearized model of the tracking error dynamics (12) can be written in discrete form as :

$$e(k+1) = A(k)e(k) + Bu_c(k) \qquad (13)$$

Where:

$$A = I + A_c(t)T_s, B = B_c T_s$$

And $A \in \mathbb{R}^{n \times n}$, n: number of states variable, $B \in \mathbb{R}^{n \times m}$ m : number of input variable and T_s : is the sampling time.

Consider the discrete-time system (13), then the following sliding mode function is defined:

$$S(k) = Ce(k) \qquad (14)$$

Where $C \in \mathbb{R}^{m \times n}$ Is the gain matrix. For a discrete-time system (13), a quasi-sliding mode reaching law is given as in [43]:

$$S(k+1) - S(k) = -q_s T_s S(k) - \varepsilon T_s \, \text{sign}(S(k)) \quad (15)$$

With : $\varepsilon > 0$, $q_s > 0$ and $1 - q_s T_s > 0$. The control law for the discrete-time system (13) can be derived by comparing (15) with (16) :

$$S(k+1) - S(k) = Ce(k+1) + Ce(k)$$
$$= CA(k)e(k) + CBu_c(k) - Ce(k) \tag{16}$$

Then, solving for $u_c(k)$ gives the following control input:

$$u_c(k) = -(CB)^{-1}[CA(k)e(k) - Ce(k) \\ + q_s T_s S(k) + \varepsilon T_s \, \text{sign}(S(k))] \tag{17}$$

3.2. Discrete predictive sliding mode control design

The main idea of predictive sliding mode control is to find a control law $u_c(k)$ that drive the predictive sliding function vector $S_p(k+1)$ to a reference sliding function vector $S_r(k+1)$, by minimizing a quadratic cost function $J_{DMPC}(u_c(k), N_p, N_c)$.

Consider the discrete sliding mode problem for the system (13), taking the reaching law (15) as a reference sliding surface results the following :

$$\begin{cases} S_r(k+\text{p}) = (1 - \text{q}_s T_s) \, S_r(k+p-1) \\ \qquad - \varepsilon T_s \, \text{sign} \, (S_r(k+p-1)) \\ S_r(k) = S(k) \end{cases} \tag{18}$$

The value of the sliding function vector (14) at time instant p can be obtained as:

$$S(k+p) = C \prod_{j=1}^{p-1} A(k+j)e(k) + \sum_{i=1}^{p} \left(C \prod_{j=1}^{p-1} A(k+j) \right)$$
$$\times B \, U_c(k+i-1) + C \, B \, U_c(k+p-1)$$

By defining the predictive sliding function S_p as follow:

$$S_p(k+1) = [S(k+1), S(k+2), \dots, S(k+N_p)]^T \tag{19}$$

Where N_p is the prediction horizon, then $S_p(k+1)$ can be described as:

$$S_p(k+1) = F(k)e(k) + H(k)U_c(k) \tag{20}$$

Where:
$$F(k) = [C \, A(k), \, C \, A(k+1)A(k), \, \dots, \, C \, \tilde{A}(k, 0)]^T$$

$$H(k) = \begin{bmatrix} CB & 0 & \cdots & 0 \\ CA(k+1)B & CB & \cdots & \vdots \\ \vdots & \vdots & \ddots & \vdots \\ C\tilde{A}(k,1) & C\tilde{A}(k,2)B(k+1) & \cdots & CB \end{bmatrix}$$

And:

$$C\tilde{A}(k, \text{i}) = C \prod_{j=\text{i}}^{p-1} A(k+j)$$

$$U_c(k) = [u_c(k), u_c(k+1), \dots, u_c(k+p)]^T$$

Then, we introduce the following cost function:

$$J_{DPSM} = \sum_{j=1}^{N_p} q_j \left(S_p(k+1) - S_r(k+j) \right)^2$$
$$+ \sum_{i=1}^{N_c} r_i \left(U_c(k) - U_{eq}(k) \right)^2 \tag{21}$$

Where $U_{eq}(k)$ is the discrete sliding mode equivalent control given by:

$$U_{eq}(k) = (CB)^{-1}[CA(k)e(k)] \tag{22}$$

The cost function in (21) can be described in quadratic form as:

$$J_{DPSM}(U_c(k), N_p, N_c) = \|(S_p(k+1) - S_r(k+1))\|_Q^2 \\ + \|(U_c(k) - U_{eq}(k))\|_R^2 \tag{23}$$

Hence, the optimal control law input $U_c(k)$ can be obtained by $\frac{dJ_{DPSM}}{dU_c} = 0$ as:

$$U_c(k) = -\left(H^T Q H + R \right)^{-1} \left[H^T (Fe(k) \;\; -S_r(k+1)) - RU_{eq} \right] \tag{24}$$

Where Q and R are weighting matrices given as:

$$Q = \begin{bmatrix} q_1 & 0 & \dots & 0 \\ 0 & q_2 & \dots & 0 \\ \vdots & \vdots & \ddots & \vdots \\ 0 & 0 & \dots & q_{N_p} \end{bmatrix}$$

$$R = \begin{bmatrix} r_1 & 0 & \dots & 0 \\ 0 & r_2 & \dots & 0 \\ \vdots & \vdots & \ddots & \vdots \\ 0 & 0 & \dots & r_{N_c} \end{bmatrix}$$

4. Simulation results

In this section, Two simulation examples are presented, a leader-follower formation control of two nonolonomic wheeled mobile robots is considered, where the first robot is assigned as a leader and the second robot is acting as follower.

The control parameters for the DSM and PDSM methods were determined by trial and error as follow : $q_s = \text{diag}[3, 0, 0, 6], \varepsilon = 0.001 \times I_{2\times2}, N_p = 4, N_c = 3, R = 10^{-3} \times I_{2\times2}, Q = \text{diag}[5, 0, 0, 5]$ and the gain matrix C is chosen as follow:

$$C = \begin{bmatrix} 1.0 & 1.4 & 0 \\ 0 & 2.4 & 1.0 \end{bmatrix}$$

$$\begin{cases} x_r = 1.5\sin(2\pi t/50) \\ y_r = 0.5\sin(4\pi t/50) \end{cases} \quad (25)$$

For the PDSM control, the limits of the velocities commands of the follower robot are given as follow:

$$\begin{cases} \nu_{f,max} = -\nu_{f,min} = 0.4m/s \\ \omega_{f,max} = -\omega_{f,min} = 1.8 Rad/s \end{cases} \quad (26)$$

While the kinematic input disturbances defined in (3) is selected as follow:

$$\Delta = \begin{bmatrix} \delta_\nu \\ \delta_\omega \end{bmatrix} = \begin{bmatrix} .01 sin(t) \\ .01 cos(t) \end{bmatrix} \quad (27)$$

4.1. Formation control using the DSM control

In this simulation example, the discrete predictive sliding mode controller (24) is used to control the formation, the leader robot is assumed to be moving in a 8-shape trajectory produced by (25). The required separation distance is chosen as $L_d = 0.15$ m and the bearing angle is selected as $\phi_d = 3\pi/2$, while the initial robots posture are given as: $q_l = [0\ 0\ \pi/4]^T$ and $q_f = [0.25\ 1.5\ -\pi/4]^T$.

The real-time trajectories for both robots are shown in Figure 3 . The follower robot tracking errors and its velocities commands are shown in Figure 4 and Figure 5, respectively.
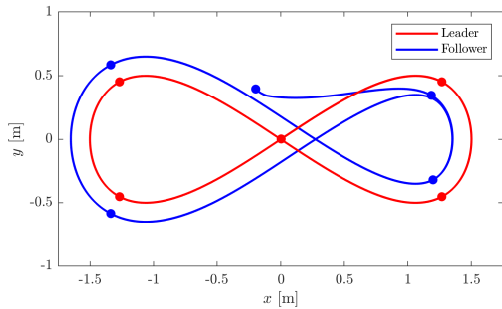

Figure 3: Two robot leader follower formation, based on the discrete predictive sliding mode DPSM control.

4.2. Comparison between DSM and DPSM control methods

This section presents a comparison between the discrete sliding mode DSM control in (17) and the discrete predictive sliding mode DPSM control in (24). In this example, the leader robot is following a circular trajectory given by equation (28) with a constant angular
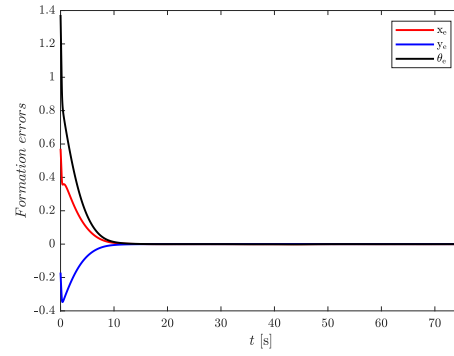

Figure 4: Formation tracking error for the follower using the discrete predictive sliding mode DPSM control controller.
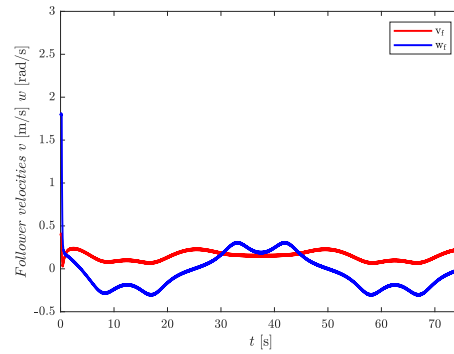

Figure 5: Control inputs of the follower robot controlled by the discrete predictive sliding mode DPSM method.

velocity $\omega_l = 1$ Rad/s and a constant linear velocity $\nu_l = 1$ m/s. The initial follower robot position is selected as $q_f = [1.2\ -1.1\ \pi/4]^T$ and the initial leader posture is $q_l = [0\ 0\ \pi/2]^T$, while the required orientation angle and distance are chosen as $L_d = 1$ m and $\phi_d = 4\pi/3$ Rad.

$$\begin{cases} x_r = -1 + \cos(2\pi t/50) \\ y_r = \sin(2\pi t/50) \end{cases} \quad (28)$$

Figure 6, shows the formation trajectories based on both DSM and DPSM control schemes. While Figure 7 depict a comparison between the formation tracking errors, and the control inputs of the follower robot using the suggested control techniques are illustrated in Figure 8

To compare the formation tracking performances, five error indexes are employed. Namely, mean square error $MSE = \frac{1}{T}\sum_1^T E_f(t)^2$, integral square error $ISE = \int_0^T E_f(t)^2 dt$, integral time square error $ITSE = \int_0^T t E_f(t)^2 dt$, integral time absolute error
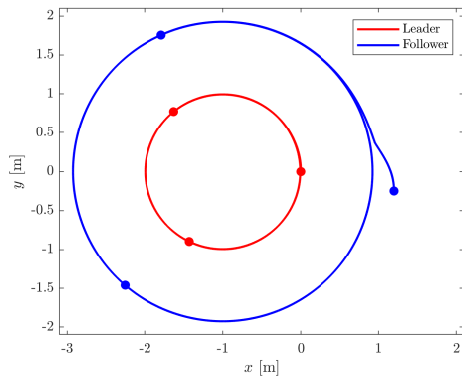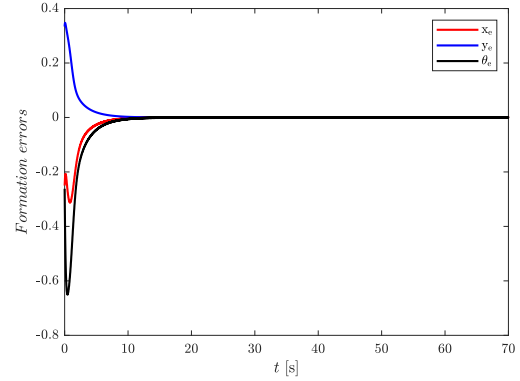
(a)
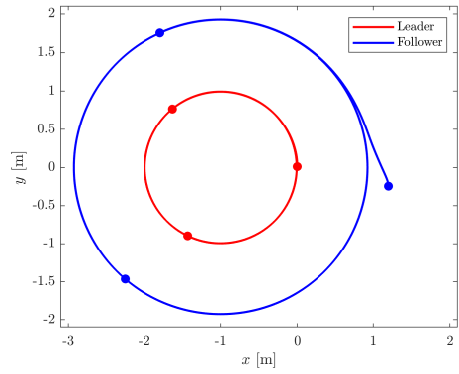
(b)

Figure 6: Comparison between the formation trajectories, (a) using the discrete sliding mode DSM controller, (b) based on the discrete predictive sliding mode PDSM controller.

(a)

(b)

Figure 7: Comparison between the tracking errors of the follower robot, (a) using the discrete sliding mode DSM controller, (b) based on the discrete predictive sliding mode PDSM controller.

$ITAE = \int_0^T t|E_f(t)|dt$, and integral absolute error $IAE = \int_0^T |E_f(t)|dt$. Where $E_f(t)$ is given in (29) and T is the time of simulation.
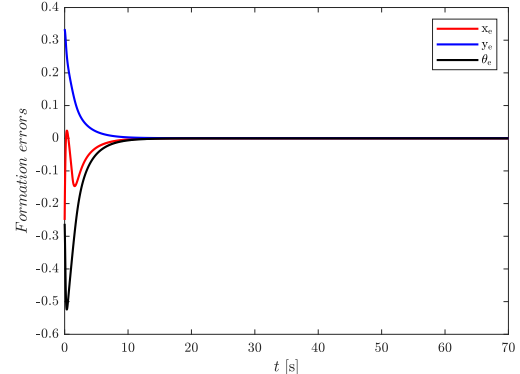
$$E_f(t) = x_e(t)^2 + y_e(t)^2 + \theta_e(t)^2 \qquad (29)$$

The obtained results of the comparison between the formation tracking performances are listed in Table 1.

In the first example, the simulation results of the leader-follower formation in an 8-shape trajectory is successfully performed. As shown in Figure 3, the follower robot effectively follows the leader, maintaining the required distance and keeping the desired heading angle. The tracking errors of the follower robot steadily decreases until it reaches zero in the presence of the input disturbances, as seen in Figure 4. Additionally, Figure 5 illustrate that the robot velocities adhere to the imposed constraints without any chattering.

The comparison between the formation trajectories in Figure 6 shows that the formation problem is successfully solved based on both proposed control strategies, where the tracking errors gradually reach the origin over time as depicted in Figure 7. However, from the control laws of the follower robots illustrated in Figure 8, it can be noted that the DPSM control scheme can generate a chattering free control signals that respect the physical input limits of the robot. Moreover, the analysis of the tracking performances in Table 1 show that DPSM control technique has a better formation tracking accuracy when compared to the DSM control strategy.

To summarize, the above simulation outcomes indicate that the proposed predictive sliding mode DPSM controller can perform an accurate formation tracking with a practical and chattering free control inputs.
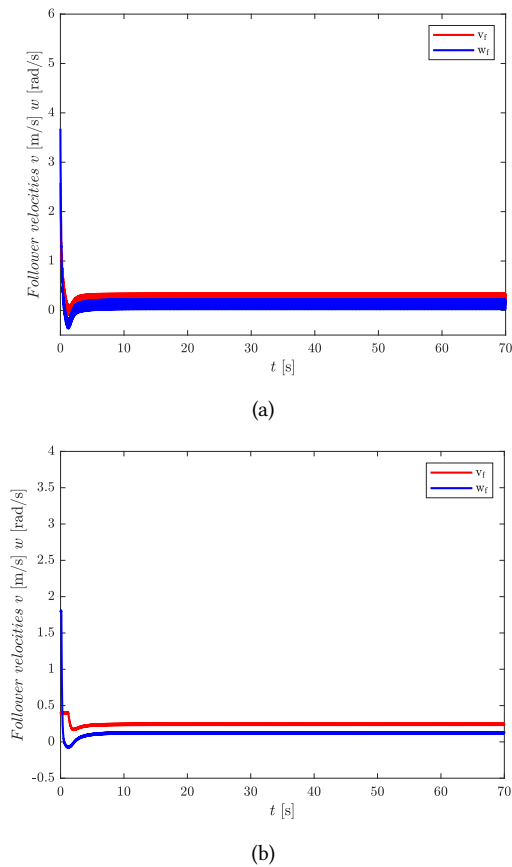
(a)

(b)

Figure 8: Comparison between the velocities signals of the follower robots, (a) using the discrete sliding mode DSM controller, (b) based on the discrete predictive sliding mode PDSM controller.

Table 1
Comparison between the formation tracking performances .

	MSE	ISE	ITSE	IAE	ITAE
DSM	0.0155	0.1211	0.0279	0.2548	0.0667
PDSM	0.0061	0.0463	0.0068	0.1528	0.0362

5. Conclusion

The leader-follower-based formation control for wheeled nonholonomic mobile robots has been addressed in this paper. Initially, the trajectory following problem was expanded into a formation control problem. Then, by the utilization of linear formation tracking error dynamics, we have designed a discrete sliding mode controller to guide the follower robots in maintaining their formation relative to the leader and achieving the desired spatial geometric configuration. Furthermore, to optimize

control efforts and mitigate the challenging chattering phenomenon, we integrated a discrete model predictive control DMPC with the DSM approach. The suggested method efficacy was demonstrated through simulation results and comparative studies.

6. Declaration on Generative AI

During the preparation of this work, the authors used ChatGPT, Grammarly in order to: Grammar and spelling check, Paraphrase and reword. After using this tool/service, the authors reviewed and edited the content as needed and take full responsibility for the publication's content.

References

[1] N. Hacene, B. Mendil, Behavior-based autonomous navigation and formation control of mobile robots in unknown cluttered dynamic environments with dynamic target tracking, International Journal of Automation and Computing (2021) 1–21.

[2] B. Nail, B. Djaidir, I. E. Tibermacine, C. Napoli, N. Haidour, R. Abdelaziz, Gas turbine vibration monitoring based on real data and neuro-fuzzy system, Diagnostyka 25 (2024).

[3] W. J. N. Goto, D. W. Bertol, N. A. Martins, Formation and trajectory tracking of mobile robots with uncertainties and disturbances using an adaptive immune fuzzy quasi-sliding mode control, Journal of Control, Automation and Electrical Systems (2024) 1–21.

[4] B. Nail, M. A. Atoussi, S. Saadi, I. E. Tibermacine, C. Napoli, Real-time synchronisation of multiple fractional-order chaotic systems: an application study in secure communication, Fractal and Fractional 8 (2024) 104.

[5] X. Chen, F. Huang, Y. Zhang, Z. Chen, S. Liu, Y. Nie, J. Tang, S. Zhu, A novel virtual-structure formation control design for mobile robots with obstacle avoidance, Applied Sciences 10 (2020) 5807.

[6] C. Napoli, V. Ponzi, A. Puglisi, S. Russo, I. Tibermacine, et al., Exploiting robots as healthcare resources for epidemics management and support caregivers, in: CEUR Workshop Proceedings, volume 3686, CEUR-WS, 2024, pp. 1–10.

[7] I. Naidji, A. Tibermacine, W. Guettala, I. E. Tibermacine, et al., Semi-mind controlled robots based on reinforcement learning for indoor application., in: ICYRIME, 2023, pp. 51–59.

[8] S. Russo, S. I. Illari, R. Avanzato, C. Napoli, Reducing the psychological burden of isolated oncological patients by means of decision trees, in: CEUR

Workshop Proceedings, volume 2768, 2020, p. 46 – 53.

[9] X. Yu, L. Liu, Leader-follower formation of vehicles with velocity constraints and local coordinate frames, Science China Information Sciences 60 (2017) 1–15.

[10] S. Bouchelaghem, I. E. Tibermacine, M. Balsi, M. Moroni, C. Napoli, Cross-domain machine learning approaches using hyperspectral imaging for plastics litter detection, in: 2024 IEEE Mediterranean and Middle-East Geoscience and Remote Sensing Symposium (M2GARSS), IEEE, 2024, pp. 36–40.

[11] G. Wen, C. P. Chen, Y.-J. Liu, Z. Liu, Neural network-based adaptive leader-following consensus control for a class of nonlinear multiagent state-delay systems, IEEE transactions on cybernetics 47 (2016) 2151–2160.

[12] N. Boutarfaia, S. Russo, A. Tibermacine, I. E. Tibermacine, Deep learning for eeg-based motor imagery classification: Towards enhanced human-machine interaction and assistive robotics, life 2 (2023) 4.

[13] C.-E. Ren, L. Chen, C. P. Chen, Adaptive fuzzy leader-following consensus control for stochastic multiagent systems with heterogeneous nonlinear dynamics, IEEE Transactions on Fuzzy Systems 25 (2016) 181–190.

[14] C.-E. Ren, C. P. Chen, Sliding mode leader-following consensus controllers for second-order non-linear multi-agent systems, IET Control Theory & Applications 9 (2015) 1544–1552.

[15] M. C. Gallotta, G. Zimatore, L. Falcioni, S. Migliaccio, M. Lanza, F. Schena, V. Biino, M. Giuriato, M. Bellafiore, A. Palma, et al., Influence of geographical area and living setting on children's weight status, motor coordination, and physical activity, Frontiers in pediatrics 9 (2022) 794284.

[16] J. Chen, D. Sun, J. Yang, H. Chen, Leader-follower formation control of multiple non-holonomic mobile robots incorporating a receding-horizon scheme, The International Journal of Robotics Research 29 (2010) 727–747.

[17] S. Russo, S. Ahmed, I. E. Tibermacine, C. Napoli, Enhancing eeg signal reconstruction in cross-domain adaptation using cyclegan, in: 2024 International Conference on Telecommunications and Intelligent Systems (ICTIS), IEEE, 2024, pp. 1–8.

[18] S. Lin, R. Jia, M. Yue, Y. Xu, On composite leader–follower formation control for wheeled mobile robots with adaptive disturbance rejection, Applied Artificial Intelligence 33 (2019) 1306–1326.

[19] S. Falciglia, F. Betello, S. Russo, C. Napoli, Learning visual stimulus-evoked eeg manifold for neural image classification, Neurocomputing 588 (2024). doi:10.1016/j.neucom.2024.127654.

[20] D. Shen, W. Sun, Z. Sun, Adaptive pid formation control of nonholonomic robots without leader's velocity information, ISA transactions 53 (2014) 474–480.

[21] C. Randieri, A. Pollina, A. Puglisi, C. Napoli, Smart glove: A cost-effective and intuitive interface for advanced drone control, Drones 9 (2025). doi:10.3390/drones9020109.

[22] S. Russo, I. E. Tibermacine, A. Tibermacine, D. Chebana, A. Nahili, J. Starczewscki, C. Napoli, Analyzing eeg patterns in young adults exposed to different acrophobia levels: a vr study, Frontiers in Human Neuroscience 18 (2024). doi:10.3389/fnhum.2024.1348154.

[23] H. Iima, Y. Kuroe, Swarm reinforcement learning methods improving certainty of learning for a multi-robot formation problem, in: 2015 IEEE Congress on Evolutionary Computation (CEC), IEEE, 2015, pp. 3026–3033.

[24] B. Ladjal, I. E. Tibermacine, M. Bechouat, M. Sedraoui, C. Napoli, A. Rabehi, D. Lalmi, Hybrid models for direct normal irradiance forecasting: A case study of ghardaia zone (algeria), Natural Hazards 120 (2024) 14703–14725.

[25] A. Tibermacine, I. E. Tibermacine, M. Zouai, A. Rabehi, Eeg classification using contrastive learning and riemannian tangent space representations, in: 2024 International Conference on Telecommunications and Intelligent Systems (ICTIS), IEEE, 2024, pp. 1–7.

[26] W. Zheng, Y. Jia, Leader-follower formation control of mobile robots with sliding mode., J. Robotics Netw. Artif. Life 4 (2017) 10–13.

[27] M. Defoort, T. Floquet, A. Kokosy, W. Perruquetti, Sliding-mode formation control for cooperative autonomous mobile robots, IEEE Transactions on Industrial Electronics 55 (2008) 3944–3953.

[28] W. J. N. Goto, N. Martins, Leader-follower formation tracking for differential-drive wheeled mobile robots with uncertainties and disturbances based on immune fuzzy quasi-sliding mode control (2023).

[29] D. Elayaperumal, Y. H. Joo, Robust swarm formation for multiple nonholonomic two-wheeled mobile robots using leader–follower approach via sliding mode controller and neural dynamic model, Journal of Electrical Engineering & Technology 18 (2023) 2245–2252.

[30] A. Alfarano, G. De Magistris, L. Mongelli, S. Russo, J. Starczewski, C. Napoli, A novel convmixer transformer based architecture for violent behavior detection, in: Lecture Notes in Computer Science (including subseries Lecture Notes in Artificial Intelligence and Lecture Notes in Bioinformatics), volume 14126 LNAI, 2023, p. 3 – 16. doi:10.1007/978-3-031-42508-0_1.

[31] S. Pepe, S. Tedeschi, N. Brandizzi, S. Russo, L. Ioc-

chi, C. Napoli, Human attention assessment using a machine learning approach with gan-based data augmentation technique trained using a custom dataset, OBM Neurobiology 6 (2022). doi:10.21926/obm.neurobiol.2204139.

[32] A. Tibermacine, D. Akrour, R. Khamar, I. E. Tibermacine, A. Rabehi, Comparative analysis of svm and cnn classifiers for eeg signal classification in response to different auditory stimuli, in: 2024 International Conference on Telecommunications and Intelligent Systems (ICTIS), IEEE, 2024, pp. 1–8.

[33] D. Gu, H. Hu, A model predictive controller for robots to follow a virtual leader, Robotica 27 (2009) 905–913.

[34] S.-M. Lee, H. Kim, H. Myung, X. Yao, Cooperative coevolutionary algorithm-based model predictive control guaranteeing stability of multirobot formation, IEEE Transactions on Control Systems Technology 23 (2014) 37–51.

[35] S. eddine Boukredine, E. Mehallel, A. Boualleg, O. Baitiche, A. Rabehi, M. Guermoui, A. Douara, I. E. Tibermacine, Enhanced performance of microstrip antenna arrays through concave modifications and cut-corner techniques, ITEGAM-JETIA 11 (2025) 65–71.

[36] N. Brandizzi, A. Fanti, R. Gallotta, S. Russo, L. Iocchi, D. Nardi, C. Napoli, Unsupervised pose estimation by means of an innovative vision transformer, in: Lecture Notes in Computer Science (including subseries Lecture Notes in Artificial Intelligence and Lecture Notes in Bioinformatics), volume 13589 LNAI, 2023, p. 3 – 20. doi:10.1007/978-3-031-23480-4_1.

[37] G. Capizzi, C. Napoli, S. Russo, M. Woźniak, Lessening stress and anxiety-related behaviors by means of ai-driven drones for aromatherapy, in: CEUR Workshop Proceedings, volume 2594, 2020, p. 7 – 12.

[38] H. Xiao, C. P. Chen, Leader-follower multi-robot formation system using model predictive control method based on particle swarm optimization, in: 2017 32nd Youth Academic Annual Conference of Chinese Association of Automation (YAC), IEEE, 2017, pp. 480–484.

[39] N. A. Martins, E. S. Elyoussef, D. W. Bertol, E. R. De Pieri, U. F. Moreno, E. B. Castelan, Nonholonomic mobile robot with kinematic disturbances in the trajectory tracking: a variable structure controller, Learning and Nonlinear Models 8 (2010) 23–40.

[40] K. L. Besseghieur, R. Trębiński, W. Kaczmarek, J. Panasiuk, Leader-follower formation control for a group of ros-enabled mobile robots, in: 2019 6th International Conference on Control, Decision and Information Technologies (CoDIT), IEEE, 2019, pp.

1556–1561.

[41] Y. Kanayama, Y. Kimura, F. Miyazaki, T. Noguchi, A stable tracking control method for a non-holonomic mobile robot., in: IROS, 1991, pp. 1236–1241.

[42] G. Klančar, I. Škrjanc, Tracking-error model-based predictive control for mobile robots in real time, Robotics and autonomous systems 55 (2007) 460–469.

[43] W. Gao, Y. Wang, A. Homaifa, Discrete-time variable structure control systems, IEEE transactions on Industrial Electronics 42 (1995) 117–122.